

Gapless spin-liquid ground state in the $S = 1/2$ kagome antiferromagnet

H. J. Liao,¹ Z. Y. Xie,^{1,2} J. Chen,¹ Z. Y. Liu,³ H. D. Xie,¹ R. Z. Huang,¹ B. Normand,^{4,2} and T. Xiang^{1,5,*}

¹*Institute of Physics, Chinese Academy of Sciences, P.O. Box 603, Beijing 100190, China*

²*Department of Physics, Renmin University of China, Beijing 100872, China*

³*Institute of Theoretical Physics, Chinese Academy of Sciences, P.O. Box 2735, Beijing 100190, China*

⁴*Laboratory for Neutron Scattering and Imaging,*

Paul Scherrer Institute, CH-5232 Villigen PSI, Switzerland

⁵*Collaborative Innovation Center of Quantum Matter, Beijing 100190, China*

(Dated: May 17, 2019)

Frustrated quantum magnetism has moved to the forefront of physics research, posing fundamental questions concerning quantum disordered states, entanglement, topology and the nature of the quantum wavefunction. The defining problem in the field is one of the simplest, the ground state of the nearest-neighbour $S = 1/2$ antiferromagnetic Heisenberg model on the kagome lattice, but has defied all theoretical and numerical methods employed to date. We apply the formalism of tensor-network states (TNS), specifically the method of projected entangled simplex states (PESS), whose combination of a correct accounting for multipartite entanglement and infinite system size provides qualitatively new insight. By studying the ground-state energy, the staggered magnetization we find at all finite tensor bond dimensions and the effects of a second-neighbour coupling, we demonstrate that the ground state is a gapless spin liquid. We discuss the comparison with other numerical studies and the physical interpretation of the gapless ground state.

In one spatial dimension, quantum fluctuations dominate any physical system and semiclassical order is destroyed. In higher dimensions, frustrated quantum magnets offer perhaps the cleanest set of systems in which to explore the possibilities for finding the same type of physics, including quantum spin-liquid states, fractionalization of spin degrees of freedom and exotic topological properties. This challenge has by now become a central focus of efforts spanning theory, numerics, experiment and materials synthesis [1–4]. While much has been understood about frustrated systems on the triangular, pyrochlore, Shastry-Sutherland and other two- and three-dimensional lattices, it is fair to say that the ground-state properties of the $S = 1/2$ antiferromagnet on the kagome geometry (depicted in Fig. 3c) with only nearest-neighbour Heisenberg interactions, $H = \sum_{\langle ij \rangle} J \vec{S}_i \cdot \vec{S}_j$, remain a complete enigma.

Analytical approaches using Schwinger bosons [5] and density-matrix renormalization-group (DMRG) calculations [6–8], including analysis of the topological entanglement entropy [9], suggest a gapped spin liquid of Z_2 topology. DMRG estimates of the triplet spin gap vary

widely with system geometry, but the most sophisticated studies [8, 10] indicate a robust gap $\Delta \geq 0.1J$. Earlier suggestions of a gapped ground state arising due to valence-bond-crystal formation have now been discarded. Analytical large- N expansions [11] and numerical simulations by the variational Monte Carlo (VMC) technique [12, 13] suggest a gapless spin liquid with $U(1)$ symmetry and a Dirac spectrum of spinons. The final conclusion from extensive exact diagonalization calculations is that the system sizes accessible by this method are simply too small to judge [14]. The debate between the gapped Z_2 and gapless $U(1)$ scenarios continues, with very recent arguments in support of both [15, 16], while a symmetry-preserving tensor-network analysis, on which we comment further below, supports the gapped Z_2 ground state [17]. The kagome antiferromagnet with further-neighbour interactions extends the space of ground states with nontrivial topology, including a chiral spin-liquid phase. None of these studies support magnetic order.

From the standpoint of materials synthesis, great strides have been made towards a pure $S = 1/2$ kagome system. $\text{ZnCu}_3(\text{OH})_6\text{Cl}_2$ (herbertsmithite) [18] offers a structurally perfect realization composed of Cu^{2+} ions. Despite the large antiferromagnetic exchange, $J \simeq 170$ – 190 K [19, 20], in experiment there is no evidence of long-ranged magnetic order or even of spin freezing at any temperature down to 50 mK [21, 22]. There is also no sign of a spin gap in the excitation spectrum of powder samples [22, 23]. Even with the availability of single crystals [24], the situation remains unresolved: neutron spectroscopy [25] shows a continuum of fractional excitations and the system was suggested to be gapless (although the upper limit was set only at $\Delta/J \leq 0.1$), but was more recently interpreted as a gapped state with correlated impurities [26]. Similarly, NMR studies have been interpreted as showing a small gap ($\Delta/J \approx 0.05$) [27], but also as providing no solid evidence for the presence of one [28]. However, the physics of herbertsmithite may in fact be controlled by Dzyaloshinskii-Moriya (DM) interactions [29–31] and, although in-plane defects [31–36] have been excluded [37], there remain possible in-plane polarization and interplane coupling effects due to out-of-plane defects. Elsewhere, candidate $S = 1/2$ kagome materials include volborthite [38] and edwardsite [39], which

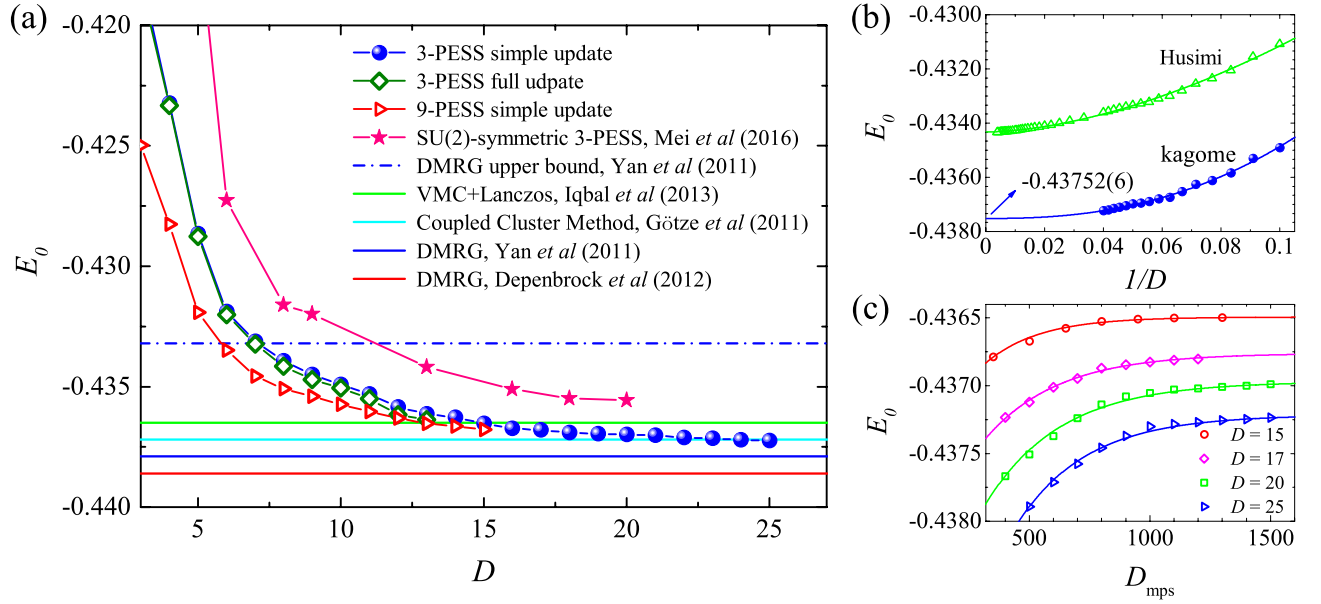


FIG. 1. **Ground-state energy of the kagome antiferromagnet.** (a) E_0 as a function of D , shown for the 3-PESS and simple-update method up to $D = 25$, 3-PESS by full update to $D = 13$ and 9-PESS with simple update to $D = 15$. Shown for comparison are the results from a wide range of different numerical studies. (b) $E_0(D)$ for the 3-PESS, shown as a function of $1/D$ and compared with results obtained for the Husimi lattice [45]. Both data sets show a similar algebraic dependence on D , which we fit by the power-law form $E_0(D) = e_0 + aD^{-\alpha}$ in order to deduce the extrapolated ground-state energy, $e_0 = -0.43752(6)$. (c) Convergence of $E_0(D)$ as a function of D_{mps} , shown for several values of D .

have distorted lattices, Cu-(1,3bdc) [40], which is ferromagnetic, and vesignieite [41] and Cd-kapellasite [42], which are known to have strong DM interactions, but all raise the pressure for a theoretical solution to the kagome problem before a definitive experimental one emerges.

To this end, we employ the PESS formulation, which we introduced in Ref. [43] and have developed subsequently, to obtain and to optimize a systematic variational Ansatz for the ground state of the model. As we discuss in the Methods section, the TNS formalism is based on expressing the wavefunction as a generalized matrix-product state (MPS), which contains local entanglement (the area law is obeyed), and constructing a renormalization-group scheme to reach the limit of infinite lattice size; the truncation parameter is the tensor bond dimension, D , which can be considered loosely as specifying the range of entanglement included in the wavefunction. The PESS approach recognizes the central role in frustrated systems of the multipartite entanglement within each lattice unit, or simplex [43–45], and allows in addition the comparison of results from different simplices. The optimized PESS approach is a projection technique, with tensor manipulation performed by higher-order singular-value decomposition, and a choice between simple- and full-update treatments of the bond environment during tensor renormalization, with the former allowing access to larger D but the latter achieving more rapid convergence.

However, TNS calculations are a two-step process, where the wavefunction is obtained first and then used to calculate physical expectation values. This latter step requires projection onto a 1D MPS basis, whose dimension for convergence is found to scale approximately as $D_{\text{mps}} \approx 4D^2$. Once $D \gtrsim 15$, the evaluation step becomes the more computationally intensive problem, and here we implement new methodology by which we extend the accessible D range to $D = 25$.

We begin by presenting our results from the 3-PESS Ansatz for all accessible D values. The ground-state energy, $E_0(D)$, of the pure kagome Heiseberg antiferromagnet is shown in Fig. 1a and lies below the estimates obtained from all known techniques other than DMRG studies of specific clusters, which do not represent an upper bound. We remark that our E_0 values are significantly lower than those of an SU(2)-invariant TNS analysis [17]. We find that $E_0(D)$ converges algebraically with D , as on the Husimi lattice [45], and the power-law fit to our results, shown in Fig. 1b, delivers our best estimate of the ground-state energy, $e_0 = -0.43752(6)J$. In Fig. 1c we illustrate the convergence of $E_0(D_{\text{mps}})$ for selected values of D ; optimized fits to a regime of exponential convergence in D_{mps} were used to extrapolate towards the values of $E_0(D)$ shown in Figs. 1a and 1b, and to determine the associated error bars, on the basis of which we limit our claims of reliability to $D \leq 25$.

One of the key qualitative properties of our PESS

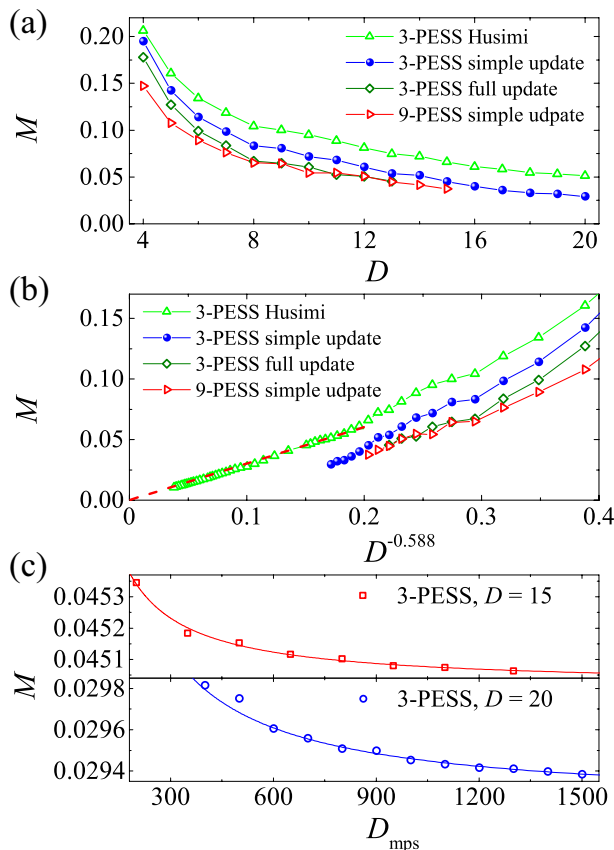


FIG. 2. **Staggered magnetization of the kagome anti-ferromagnet at finite values of D .** (a) M as a function of D , shown for the 3-PESS and simple-update method up to $D = 20$, 3-PESS by full update to $D = 13$ and 9-PESS with simple update to $D = 15$. Shown for comparison are results obtained for the Husimi lattice [45]. (b) M as a function of $1/D^{0.588}$, the power-law form obtained for the Husimi lattice. (c) Convergence of $M(D)$ as a function of D_{mps} , shown for $D = 15$ and $D = 20$.

wavefunction is that the ground state always has a finite degree of 120° magnetic order at finite values of D , as shown in Fig. 2a. The order parameter, $M(D)$, is always smaller than the analogous results for the Husimi lattice and also appears to vanish algebraically with $1/D$, as shown in Fig. 2b. Figure 2c illustrates the convergence of $M(D_{\text{mps}})$ for $D = 15$ and 20 , where an algebraic convergence with D_{mps} was deduced by considering the truncation error, and reliable extrapolations to the limit of large D_{mps} were obtained only for $D \leq 20$.

We stress that the Husimi lattice provides essential confirmation of a number of our results. It possesses exactly the same local physics as the kagome lattice but less frustration from longer paths, and allows PESS calculations to be performed up to $D = 260$, yielding accurate extrapolations to the large- D limit [45]. It confirms the crucial qualitative statement that magnetically ordered states have the lowest energies (cf. Ref. [17]) for

spatially infinite systems at finite D . It benchmarks the algebraic nature of $E_0(D)$ and $M(D)$ and also sets an upper bound on $M(D)$, well beneath which the kagome results lie. Thus we conclude that, as for Husimi, the ground state on the kagome lattice is a gapless spin liquid.

A rigorous demonstration of this conclusion requires the consideration of every aspect of the PESS procedure. Full-update calculations confirm the accuracy of the simple-update approximation for all accessible values of D : they find only slightly lower values of $E_0(D)$ (Fig. 1a), as one may expect of a more efficient technique, and no change in functional form; similarly, $M(D)$ is suppressed by several percent (Figs. 2a and 2b), reinforcing the argument for convergence to $M = 0$ at large D and still showing algebraic behaviour. To investigate whether magnetic order might be artificially enhanced by the 3-PESS, in Figs. 1a, 2a and 2b we have also shown the results obtained from a 9-PESS, which again confirm the algebraic form of $E_0(D)$ and $M(D)$, with no evidence either of a crossover to exponential behaviour of $E_0(D)$ or of a collapse of $M(D)$ to zero at finite D .

Further essential confirmation is obtained by adding a next-neighbour coupling, J_2 . Calculations with a J_2 interaction require a nine-site simplex (9-PESS) and we reach $D = 15$ within the simple-update approach. The ground-state energy and magnetization are shown in Fig. 3. $E_0(J_2)$ is maximal, meaning the system is most frustrated, close to $J_2 = 0$ and is not symmetrical about this point (Fig. 3a). For the Husimi lattice, we find a continuous evolution for all J_2 and maximal frustration at $J_2 \simeq 0.04$. By contrast, $E_0(J_2)$ for the kagome lattice shows a regime of almost constant energy when $-0.03 \lesssim J_2 \lesssim 0.04$ (Fig. 3b). To understand the nature of these phases, we consider in Fig. 3c the finite- D magnetization and in Fig. 3d $M(D)$ for selected values of J_2 . For the Husimi lattice, $M(J_2)$ is zero only at $J_2 = 0$, where it has a discontinuity, and [despite the form of $E_0(J_2)$] is almost symmetrical about this point. For the kagome lattice, the ordered phases are expected to be the $q = 0$ structure at $J_2 > 0$ and the $\sqrt{3} \times \sqrt{3}$ structure at $J_2 < 0$; both are represented schematically in Fig. 3c. However, $M(J_2)$ at finite D continues to fall through $J_2 = 0$ from above, indicating a finite regime of $q = 0$ order at $J_2 < 0$, which is terminated at $J_2 \simeq -0.03$ by a first-order transition to $\sqrt{3} \times \sqrt{3}$ order. From Fig. 3d, $M(D)$ appears to extrapolate to zero over a range of J_2 values, which we estimate from the Husimi magnetization to be fully consistent with the “plateau” in $E(J_2)$ (Fig. 3b).

In the Husimi case, we find magnetically ordered systems at all finite values of $|J_2|$, with a gapless spin liquid appearing only at the single point $J_2 = 0$, a type of “phase diagram” allowed on the pathological Husimi geometry. In the kagome case, the phase diagram is expected to contain a gapless spin liquid over a finite range

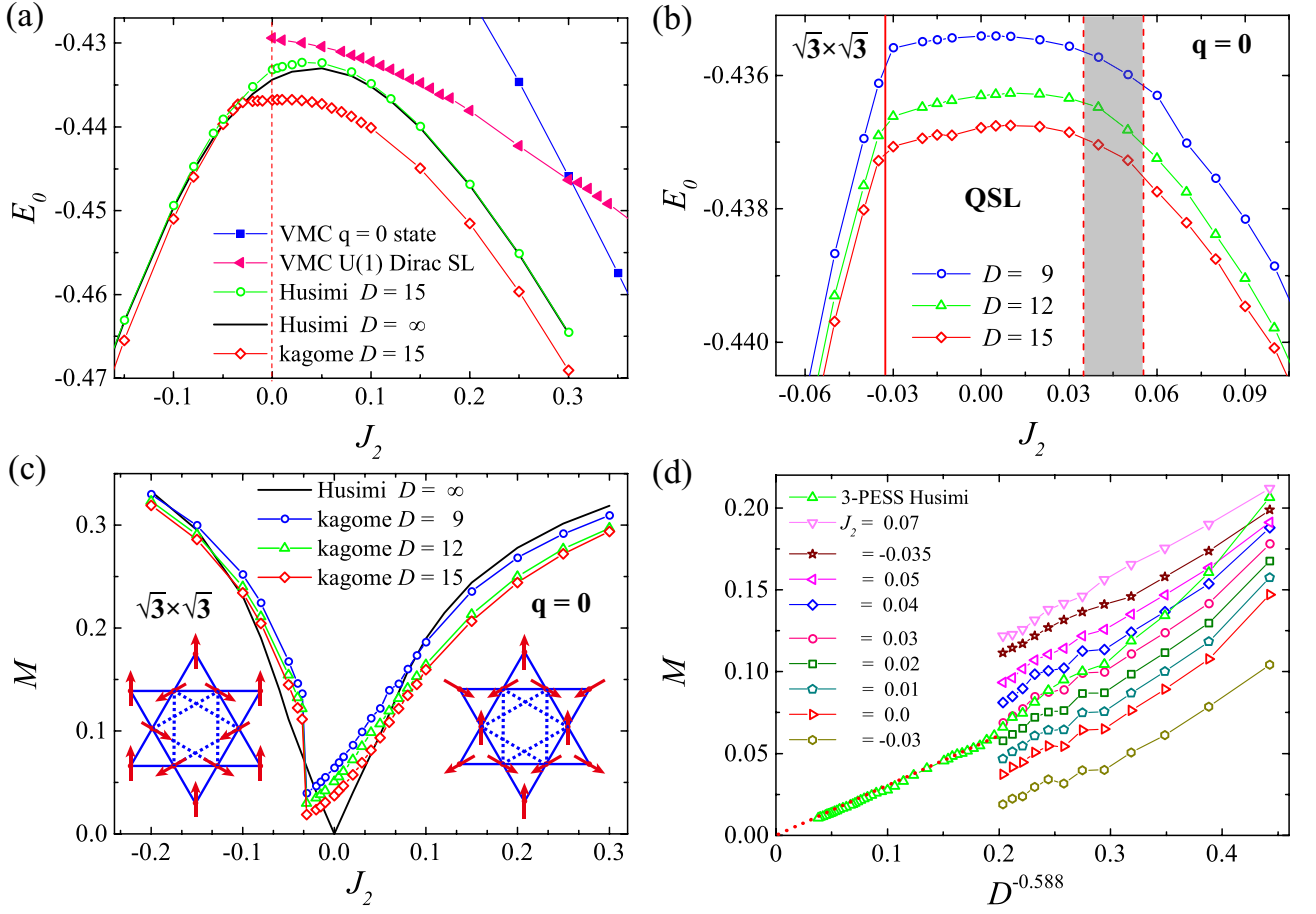


FIG. 3. **Energy and staggered magnetization of the kagome antiferromagnet with next-neighbour coupling.** (a) Ground-state energy of the kagome lattice as a function of J_2 , calculated with a 9-PSS using $D = 15$. Shown for comparison are the analogous results for the Husimi lattice with $D = 15$ and $D = \infty$, as well as the VMC results of Ref. [13]. (b) Detail of $E_0(J_2)$ near $J_2 = 0$, showing the emergence with increasing D of a cusp-type discontinuity near $J_2 = -0.03$ (red solid line). The shaded region denotes the uncertainty in the location of the continuous transition at small positive J_2 , deduced from the magnetization of panel (d). (c) Staggered magnetization, $M(J_2)$, calculated using $D = 9, 12$ and 15 , with analogous results for the Husimi lattice with $D = \infty$. Insets represent the $\sqrt{3} \times \sqrt{3}$ (left) and $q = 0$ (right) ordered phases, which are the respective ground states at sufficiently large negative and positive J_2 ; solid lines denote nearest-neighbour (J) bonds and dashed lines the next-neighbour ones (J_2). (d) Magnetization as a function of $1/D^{0.588}$, indicating the J_2 values for which M may extrapolate to zero within the error bars.

of J_2 if this is a robust quantum ground state. Indeed we find such a regime, bounded by a first-order transition at $J_2 \simeq -0.03$ and an apparent second-order transition at $J_2 = 0.045 \pm 0.01$. Evidently the additional quantum fluctuations arising due to the presence of geometrical loops in the kagome system act to create a QSL ground state with exactly the gapless characteristics of the nearest-neighbour model ($J_2 = 0$, Figs. 1 and 2). Our results are in qualitative accord with those proposed in Ref. [13] on the basis of VMC studies of a finite system, but from a quantitative standpoint the range of QSL stability we deduce is much narrower.

Concerning the calculation of other types of expectation value, regrettably the field-induced magnetization contains no useful information about the ground state be-

cause the system is ordered at finite D . Similarly, finite- D correlation functions do not contain any evidence of the nontrivial power-law behaviour expected in a gapless spin liquid when superposed on the constant part. We have nevertheless obtained definitive numerical results for the two most characteristic quantities, $E_0(D, J_2)$ and $M(D, J_2)$, for systems of infinite size by a method which, although based on gapped tensor-product states, has the capability to indicate its own “breakdown” in the event of continuing algebraic convergence. Thus the conclusion of a gapless spin-liquid ground state is robust.

To interpret this result, we begin by considering its physical implications. The leading candidate gapless wavefunction is the U(1) Dirac-fermion state proposed in Ref. [11]. While we cannot exclude one of the possible

gapless Z_2 spin-liquid states of the kagome system [46], there is currently neither numerical evidence [13] nor a physical argument in support of these. Heuristically, the formation of gapped spin liquids is favoured by the presence of low-energy local states, such as dimer- or plaquette singlets, whereas systems with a net odd-half-integer spin per simplex do not offer this option. Our results imply that there is no meaningful larger unit (such as the 12-site, six-pointed star around a single hexagon) on the kagome lattice. Instead the system optimizes its energy by maximizing the kinetic energy of mobile spinons, leading to the $U(1)$ Dirac-fermion state, or by maximizing the contributions from gauge fluctuations [47]. The gapless spin liquid is expected to have long-ranged entanglement and correlation functions [48], and the $U(1)$ state has no well-characterized topological order.

Turning to the general question of numerical studies of the kagome antiferromagnet, our results constitute a major breakthrough because of the infinite system size. A further key feature is that, although we use an MPS formalism, it is capable of indicating its own breakdown in that convergence remains algebraic instead of turning exponential. The fact that all ED and DMRG studies consistently favour gapped spin-liquid states suggests strongly that systems finite even in only one of their dimensions are not able to account appropriately for spinon kinetic-energy contributions. Regarding the question of enforced or emerging spin symmetries, PESS studies enforcing $U(1)$ [49] or $SU(2)$ [17] symmetry find spin-liquid states that have higher energies than ours at finite D (Fig. 1). It is also straightforward within the PESS technique to start with a gapped trial wavefunction and show that an ordered state of lower energy emerges on projection when D is finite. Thus it appears that studies enforcing a chosen symmetry are finding excited states of the system rather than conducting an unbiased assessment of the true ground state. It is likely that the same applies to studies on systems of finite size, and indeed it is argued in Ref. [16] that a gapped Z_2 ground state can lie at lower energy than the gapless $U(1)$ state on a finite system, but not in the thermodynamic limit.

It remains true that the kagome antiferromagnet is a problem where competing states of very different character lie very close in energy. One may equally ask why the large- N approach is correct, and here we deduce that it offers the best theoretical account for the effects of quantum fluctuations, specifically by capturing the kinetic-energy gain of mobile spinons. Our results also demonstrate the qualitative accuracy of the VMC calculations [13], despite their size limitations; we note also that the VMC approach arrives at the gapless spin-liquid ground state by a different route from PESS, without allowing states of finite magnetization. As above, it is also essential to benchmark whether the PESS Ansatz is “neutral” in its energy accounting, and does not over-emphasize gapless or ordered states, a question we addressed by

comparing the 3- and 9-PESS results in Figs. 1a and 2a.

A further question concerns the possibility that the algebraic behaviour we observe could cross over to exponential convergence beyond the range of our PESS calculations. If such a crossover were to begin at $D = 26$, it is hard to argue (consider Fig. 1b) that the difference in extrapolated ground-state energies could exceed $\Delta E = 0.0001J$. This miniscule energy would have to be the spin gap of the corresponding Z_2 state, but clearly lies far below the DMRG gap. One is then faced with the emergence of an extremely small energy scale for no apparent reason: such a value lies well below the “stabilization energy” of any of the competing states, whether this be due to local resonances, spinon kinetic energy, gauge fluctuations or any other mechanism.

Returning briefly to experiment, studies of herbertsmithite have indeed suggested a continuum of fractional spin excitations, but some of the most recent studies face competing gapped [26, 27] and gapless [25, 28] interpretations. However, it remains unclear, due to interplane disorder and DM interactions, whether this material is providing a true reflection of kagome physics.

In summary, we have used the method of projected entangled simplex states to demonstrate that the ground state of the Heisenberg antiferromagnet for $S = 1/2$ spins on the kagome lattice with only nearest-neighbour interactions is a gapless quantum spin liquid. A finite next-neighbour interaction reveals the presence of a narrow regime of gapless spin liquid between states of finite 120-degree staggered magnetic order. This spin liquid is thought to be the $U(1)$ Dirac-fermion state, in which the primary driving force for spin-liquid behaviour is the maximization of spinon kinetic energy.

Methods

The TNS approach [50–52] allows direct access to the thermodynamic limit of a physical system, respects by construction the area law of entanglement entropy [53] and is free of any sign problem [54]. The PESS Ansatz [43] allows its full and efficient application to strongly frustrated systems. The PESS representation is determined by imaginary-time evolution [55] with an arbitrary starting wavefunction. It is truncated by the tensor bond dimension, D , the number of the auxiliary virtual degrees of freedom [43, 52] introduced on each lattice bond to describe the local physical degrees of freedom, with larger D ensuring a more accurate representation.

In updating the PESS wavefunction after each projection step (implemented as a small time step), one may attempt to include the full system, or bond environment, in a self-consistent manner by the full-update (FU) [57] scheme, or neglect it within the simple-update (SU) approach [43, 56], where the bond update corresponds to a (computationally more tractable) global optimization problem. SU is exact in 1D and on the Husimi lattice, where the bonds have no additional environment

[45, 58]. Figures 1a and 2a compare the values of E_0 and M obtained by the SU and FU techniques. The SU approach clearly overestimates the expectation value of a local observable, and can be regarded as providing an upper bound. However, the key information is that the computational cost of the FU approach prohibits its use beyond $D = 13$, whereas SU can be employed to at least double this value. Because the behaviour of E_0 and M obtained by SU is very similar to the more efficient FU, and the much greater D delivers far superior estimates of both (Figs. 1a and 2a), we rely on SU for our primary conclusions. We also gauge the effects of the simplex itself by comparing our results from the 3-PESS and 9-PESS Ansätze (Figs. 1a and 2a).

The calculation of a physical expectation value from a PESS representation with bond dimension D requires in general the full summation over a two-dimensional reduced tensor network with bond dimension D^2 . This becomes the primary bottleneck at larger D in most tensor-network algorithms [59]. We have developed a new approach to this problem, which is based on the conventional time-evolving block decimation (TEBD) technique for performing the summation [60] but avoids calculating the reduced tensor network by obtaining the expectation values directly from the local tensors in the PESS representation [61]. By comparison with the TEBD method in two dimensions, the new method reduces both the computational and memory costs by two orders of D , i.e. from D^{10} to D^8 and from D^8 to D^6 respectively. Thus we are able to extend the calculation of some expectation values as far as $D = 30$ ($D = 25$ with full statistical reliability, which we gauge by considering the truncation error for given D_{mps}). This extended range is very important for the kagome Heisenberg antiferromagnet because of the very slow convergence of $E_0(D)$ and $M(D)$ (Figs. 1a, 1b and Fig. 2a).

* txiang@iphy.ac.cn

- [1] Balents, L. Spin liquids in frustrated magnets. *Nature* **464**, 199-208 (2010).
- [2] Mendels, P. & Wills, A. S. *Introduction to Frustrated Magnetism Ch. 9*, eds. Lacroix, C., Mendels, P. & Mila, F. (Springer, Heidelberg, 2011).
- [3] Kanoda, K. & Kato, R. Mott Physics in Organic Conductors with Triangular Lattices. *Annu. Rev. Condens. Matter Phys.* **2**, 167-188 (2011).
- [4] Normand, B. Frontiers in frustrated magnetism. *Con-temp. Phys.* **50**, 4, 533-552 (2009).
- [5] Sachdev, S. Kagomé- and triangular-lattice Heisenberg antiferromagnets: Ordering from quantum fluctuations and quantum-disordered ground states with unconfined bosonic spinons. *Phys. Rev. B* **45**, 12377-12396 (1992).
- [6] Jiang, H. C., Weng, Z. Y. & Sheng, D. N. Density Matrix Renormalization Group Numerical Study of the Kagome Antiferromagnet. *Phys. Rev. Lett.* **101**, 117203 (2008).
- [7] Yan, S., Huse, D. A. & White, S. R. Spin-Liquid Ground State of the $S = 1/2$ Kagome Heisenberg Antiferromagnet. *Science* **332**, 1173-1176 (2011).
- [8] Depenbrock, S., McCulloch, I. P. & Schollwöck, U. Nature of the Spin-Liquid Ground State of the $S = 1/2$ Heisenberg Model on the Kagome Lattice. *Phys. Rev. Lett.* **109**, 067201 (2012).
- [9] Jiang, H. C., Wang, Z. H. & Balents, L. Identifying topological order by entanglement entropy. *Nat. Phys.* **8**, 902-905 (2012).
- [10] Nishimoto, S., Shibata, N. & Hotta, C. Controlling frustrated liquids and solids with an applied field in a kagome Heisenberg antiferromagnet. *Nat. Commun.* **4**, 2287 (2013).
- [11] Ran, Y., Hermele, M., Lee, P. A. & Wen, X. G. Projected-Wave-Function Study of the Spin-1/2 Heisenberg Model on the Kagomé Lattice. *Phys. Rev. Lett.* **98**, 117205 (2007).
- [12] Iqbal, Y., Becca, F., Sorella, S. & Poilblanc, D. Gapless spin-liquid phase in the kagome spin- $\frac{1}{2}$ Heisenberg antiferromagnet. *Phys. Rev. B* **87**, 060405(R) (2013).
- [13] Iqbal, Y., Poilblanc, D. & Becca, F. Spin- $\frac{1}{2}$ Heisenberg J_1 - J_2 antiferromagnet on the kagome lattice. *Phys. Rev. B* **91**, 020402(R) (2015).
- [14] Sindzingre, P. & Lhuillier, C. Low-energy excitations of the kagomé antiferromagnet and the spin-gap issue. *Eur. Phys. Lett.* **88**, 27009 (2009).
- [15] Li, T. Z_2 spin liquid phase on the kagome lattice: a new saddle point. unpublished (arXiv:1601.02165).
- [16] Iqbal, Y., Poilblanc, D. & Becca, F. Comment on "Z₂ spin liquid phase on the kagome lattice: a new saddle point", by Tao Li [arXiv:1601.02165 (2016)]. unpublished (arXiv:1606.02255).
- [17] Mei, J. W., Chen, J. Y., He, H. & Wen, X. G. SU(2) spin-rotation symmetric tensor network state for spin-1/2 Heisenberg model on kagome lattice and its modular matrices. unpublished (arXiv:1606.09639).
- [18] Shores, M. P., Nytko, E. A., Bartlett, B. M. & Nocera, D. G. A Structurally Perfect $S = 1/2$ Kagomé Antiferromagnet. *J. Am. Chem. Soc.* **127**, 13462-13463 (2005).
- [19] Rigol, M. & Singh, R. R. P. Magnetic Susceptibility of the Kagome Antiferromagnet $\text{ZnCu}_3(\text{OH})_6\text{Cl}_2$. *Phys. Rev. Lett.* **98**, 207204 (2007).
- [20] Misguich, G. & Sindzingre, P. Magnetic susceptibility and specific heat of the spin- $\frac{1}{2}$ Heisenberg model on the kagome lattice and experimental data on $\text{ZnCu}_3(\text{OH})_6\text{Cl}_2$. *Eur. Phys. J. B* **59**, 305-309 (2007).
- [21] Mendels, P., Bert, F., de Vries, M. A., Olariu, A., Harrison, A., Duc, F., Trombe, J. C., Lord, J. S., Amato, A. & Baines, C. Quantum Magnetism in the Paratacamite Family: Towards an Ideal Kagomé Lattice. *Phys. Rev. Lett.* **98**, 077204 (2007).
- [22] Helton, J. S., Matan, K., Shores, M. P., Nytko, E. A., Bartlett, B. M., Yoshida, Y., Takano, Y., Suslov, A., Qiu, Y., Chung, J.-H., Nocera, D. G. & Lee, Y. S. Spin Dynamics of the Spin-1/2 Kagome Lattice Antiferromagnet $\text{ZnCu}_3(\text{OH})_6\text{Cl}_2$. *Phys. Rev. Lett.* **98**, 107204 (2007).
- [23] Olariu, A., Mendels, P., Bert, F., Duc, F., Trombe, J. C., de Vries, M. A. & Harrison, A. ^{17}O NMR Study of the Intrinsic Magnetic Susceptibility and Spin Dynamics of the Quantum Kagome Antiferromagnet $\text{ZnCu}_3(\text{OH})_6\text{Cl}_2$. *Phys. Rev. Lett.* **100**, 087202 (2008).
- [24] Han, T. H., Helton, J. S., Chu, S., Prodi, A., Singh, D. K., Mazzoli, C., Müller, P., Nocera, D. G. &

- Lee, Y. S. Synthesis and characterization of single crystals of the spin- $\frac{1}{2}$ kagome-lattice antiferromagnets $\text{Zn}_x\text{Cu}_{4-x}(\text{OH})_6\text{Cl}_2$. *Phys. Rev. B* **83**, 100402(R) (2011).
- [25] Han, T. H., Helton, J. S., Chu, S. Y., Nocera, D. G., Rodriguez-Rivera, J. A., Broholm, C. & Lee, Y. S. Fractionalized excitations in the spin-liquid state of a kagome-lattice antiferromagnet. *Nature* **492**, 406-410 (2012).
- [26] Han, T. H., Norman, M. R., Wen, J. J., Rodriguez-Rivera, J. A., Helton, J. S., Broholm, C. & Lee, Y. S. Correlated impurities and intrinsic spin-liquid physics in the kagome material herbertsmithite. *Phys. Rev. B* **94**, 060409 (2016).
- [27] Fu, M. X., Imai, T., Han, T. H. & Lee, Y. S. Evidence for a gapped spin-liquid ground state in a kagome Heisenberg antiferromagnet. *Science* **350**, 655-658 (2015).
- [28] Khuntia, P. *et al.*, unpublished.
- [29] Zorko, A., Nellutla, S., van Tol, J., Brunel, L. C., Bert, F., Duc, F., Trombe, J. C., de Vries, M. A., Harrison, A. & Mendels, P. Dzyaloshinskii-Moriya Anisotropy in the Spin-1/2 Kagome Compound $\text{ZnCu}_3(\text{OH})_6\text{Cl}_2$. *Phys. Rev. Lett.* **101**, 026405 (2008).
- [30] Cépas, O., Fong, C. M., Leung, P. W. & Lhuillier, C. Quantum phase transition induced by Dzyaloshinskii-Moriya interactions in the kagome antiferromagnet. *Phys. Rev. B* **78**, 140405(R) (2008).
- [31] Rousochatzakis, I., Manmana, S., Läuchli, A., Normand, B. & Mila, F. Dzyaloshinskii-Moriya anisotropy and nonmagnetic impurities in the $s=\frac{1}{2}$ kagome system $\text{ZnCu}_3(\text{OH})_6\text{Cl}_2$. *Phys. Rev. B* **79**, 214415 (2009).
- [32] Dommange, S., Mambrini, M., Normand, B. & Mila, F. Static impurities in the $S = 1/2$ kagome lattice: Dimer freezing and mutual repulsion. *Phys. Rev. B* **68**, 224416 (2003).
- [33] Läuchli, A., Dommange, S., Normand, B. & Mila, F. Static impurities in the $S=\frac{3}{2}$ kagome lattice: Exact diagonalization calculations on small clusters. *Phys. Rev. B* **76**, 144413 (2007).
- [34] Lee, S. H., Kikuchi, H., Qiu, Y., Lake, B., Huang, Q., Habicht, K. & Kiefer, K. Quantum-spin-liquid states in the two-dimensional kagome antiferromagnets $\text{Zn}_x\text{Cu}_{4-x}(\text{OH})_6\text{Cl}_2$. *Nat. Mater.* **6**, 853-857 (2007).
- [35] de Vries, M. A., Kamenev, K. V., Kockelmann, W. A., Sanchez-Benitez, J. & Harrison, A. Magnetic Ground State of an Experimental $S = 1/2$ Kagome Antiferromagnet. *Phys. Rev. Lett.* **100**, 157205 (2008).
- [36] Bert, F., Nakamae, S., Ladiou, F., L'Hôte, D., Bonville, P., Duc, F., Trombe, J. C. & Mendels, P. Low temperature magnetization of the $S = \frac{1}{2}$ kagome antiferromagnet $\text{ZnCu}_3(\text{OH})_6\text{Cl}_2$. *Phys. Rev. B* **76**, 132411 (2007).
- [37] Freedman, D. E., Han, T. H., Prodi, A., Müller, P., Huang, Q. Z., Chen, Y. S., Webb, S. M., Lee, Y. S., McQueen, T. M. & Nocera, D. G. Site Specific X-ray Anomalous Dispersion of the Geometrically Frustrated Kagomé Magnet, Herbertsmithite, $\text{ZnCu}_3(\text{OH})_6\text{Cl}_2$. *J. Am. Chem. Soc.* **132**, 16185-16190 (2010).
- [38] Hiroi, Z., Hanawa, M., Kobayashi, N., Nohara, M., Takagi, H., Kato, Y. & Takigawa, M. Spin-1/2 Kagomé-Like Lattice in Volborthite $\text{Cu}_3\text{V}_2\text{O}_7(\text{OH})_2 \cdot 2\text{H}_2\text{O}$. *J. Phys. Soc. Jpn.* **70**, 3377-3384 (2001).
- [39] Ishikawa, H., Okamoto, Y. & Hiroi, Z. Magnetic Properties of the Spin-1/2 Deformed Kagome Antiferromagnet Edwardsite. *J. Phys. Soc. Jpn.* **82**, 063710 (2013).
- [40] Nytko, E. A., Helton, J. S., Müller, P. & Nocera, D. G. A Structurally Perfect $S = 1/2$ Metal-Organic Hybrid Kagomé Antiferromagnet. *J. Am. Chem. Soc.* **130**, 2922-2923 (2008).
- [41] Okamoto, Y., Yoshida, H. & Hiroi, Z. Vesignieite $\text{BaCu}_3\text{V}_2\text{O}_8(\text{OH})_2$ as a Candidate Spin-1/2 Kagome Antiferromagnet. *J. Phys. Soc. Jpn.* **78**, 033701 (2009).
- [42] Oswald, H. R. Kristallstruktur von Cadmium-Kupfer-Hydroxidnitrat, $\text{CdCu}_3(\text{OH})_6(\text{NO}_3)_2 \cdot \text{H}_2\text{O}$. *Helv. Chim. Acta.* **52**, 2369-2380 (1969).
- [43] Xie, Z. Y., Chen, J., Yu, J. F., Kong, X., Normand, B. & Xiang, T. Tensor Renormalization of Quantum Many-Body Systems Using Projected Entangled Simplex States. *Phys. Rev. X* **4**, 011025 (2014).
- [44] Arovas, D. P. Simplex solid states of $\text{SU}(N)$ quantum antiferromagnets. *Phys. Rev. B* **77**, 104404 (2008).
- [45] Liao, H. J., Xie, Z. Y., Chen, J., Han, X. J., Xie, H. D., Normand, B. & Xiang, T. Heisenberg antiferromagnet on the Husimi lattice. *Phys. Rev. B* **93**, 075154 (2016).
- [46] Lu, Y. M., Ran, Y. & Lee, P. A. Z_2 spin liquids in the $S = \frac{1}{2}$ Heisenberg model on the kagome lattice: A projective symmetry-group study of Schwinger fermion mean-field states. *Phys. Rev. B* **83**, 224413 (2011).
- [47] He, Y. C., Fuji, Y. & Bhattacharjee, S. Kagome spin liquid: a deconfined critical phase driven by $\text{U}(1)$ gauge fluctuation. unpublished (arXiv:1512.05381).
- [48] Hermele, M., Ran, Y., Lee, P. A. & Wen, X. G. Properties of an algebraic spin liquid on the kagome lattice. *Phys. Rev. B* **77**, 224413 (2008).
- [49] Li, W. private communication.
- [50] Niggemann, H., Klümper, A. & Zittartz, J. Quantum phase transition in spin-3/2 systems on the hexagonal lattice – optimum ground state approach. *Z. Phys. B* **104**, 103-110 (1997).
- [51] Nishino, T., Hieida, Y., Okunishi, K., Maeshima, N., Akutsu, Y. & Gendiar, A. Two-Dimensional Tensor Product Variational Formulation. *Prog. Theor. Phys.* **105**, 409-417 (2001).
- [52] Verstraete, F. & Cirac, J. I. Renormalization algorithms for Quantum-Many Body Systems in two and higher dimensions. unpublished (arXiv:cond-mat/0407066).
- [53] Eisert, J., Cramer, M. & Plenio, M. B. Colloquium: Area laws for the entanglement entropy. *Rev. Mod. Phys.* **82**, 277-306 (2010).
- [54] Nightingale, M. P. & Umrigar, J. C. *Quantum Monte Carlo Methods in Physics and Chemistry* (Springer, Heidelberg, 1999).
- [55] Vidal, G. Efficient Classical Simulation of Slightly Entangled Quantum Computations. *Phys. Rev. Lett.* **91**, 147902 (2003); Vidal, G. Efficient Simulation of One-Dimensional Quantum Many-Body Systems. *Phys. Rev. Lett.* **93**, 040502 (2004).
- [56] Jiang, H. C., Weng, Z. Y. & Xiang, T. Accurate Determination of Tensor Network State of Quantum Lattice Models in Two Dimensions. *Phys. Rev. Lett.* **101**, 090603 (2008).
- [57] Lubasch, M., Cirac, J. I. & Banuls, M. C. Algorithms for finite projected entangled pair states. *Phys. Rev. B* **90**, 064425 (2014); Phien, H. N., Benghua, J. A., Tuan, H. D., Corboz, P. & Orús, R. Infinite projected entangled pair states algorithm improved: Fast full update and gauge fixing. *Phys. Rev. B* **92**, 035142 (2015).
- [58] Li, W., Von Delft, J. & Xiang, T. Efficient simulation of infinite tree tensor network states on the Bethe lattice. *Phys. Rev. B* **86**, 195137 (2012).
- [59] Zhao, H. H., Xie, Z. Y., Chen, Q. N., Wei, Z. C., Cai,

- J. W. & Xiang, T. Renormalization of tensor-network states. *Phys. Rev. B* **81**, 174411 (2010); Orus, R. A practical introduction to tensor networks: Matrix product states and projected entangled pair states. *Ann. Phys.* **349**, 117-158 (2014).
- [60] Vidal, G. Classical Simulation of Infinite-Size Quantum Lattice Systems in One Spatial Dimension. *Phys. Rev. Lett.* **98**, 070201 (2007); Orús, R. & Vidal, G. Infinite time-evolving block decimation algorithm beyond unitary evolution. *Phys. Rev. B* **78**, 155117 (2008); Jordan, J., Orus, R., Vidal, G., Verstraete, F. & Cirac, J. I. Classical Simulation of Infinite-Size Quantum Lattice Systems in Two Spatial Dimensions. *Phys. Rev. Lett.* **101**, 250602 (2008).
- [61] Xie, Z. Y., Liao, H. J., Liu, Z. Y., Huang, R. Z., Xie, H. D., Chen, J. & Xiang, T. unpublished.

Acknowledgements

We thank L. Balents, F. Becca, M. Hermele and W. Li for helpful discussions. This work was supported by the National Natural Science Foundation of China

(Grant Nos. 10934008, 10874215, and 11174365) and by the National Basic Research Program of China (Grant Nos. 2012CB921704 and 2011CB309703).

Author contributions

Primary programming development and data acquisition were carried out by H.J.L. and Z.Y.X. J.C., Z.Y.L., H.D.X. and R.Z.H. assisted with numerical development and data gathering. The numerical framework was conceived by Z.Y.X. and T.X. The theoretical framework was conceived by B.N. and T.X. Data refinement and figure preparation were performed by H.J.L. and Z.Y.X. The text was written by H.J.L., Z.Y.X., B.N. and T.X.

Additional information

Reprints and permissions information is available at www.nature.com/reprints. The authors declare no competing financial interests. Correspondence and requests for materials should be addressed to T.X. (txiang@iphy.ac.cn).